



# Enhanced cathode performance of nano-sized lithium iron phosphate composite using polytetrafluoroethylene as carbon precursor



Ercan Avci\*

TUBITAK, Marmara Research Center Energy Institute, 41470 Gebze, Kocaeli, Turkey

## HIGHLIGHTS

- Pyrolysis of PTFE promotes cathode performance.
- Fluorine-free carbon layer on  $\text{LiFePO}_4$  particles are formed.
- PTFE restricts the  $\text{LiFePO}_4$  particle growth.
- PTFE shifts the particle size distribution to the nanometer region.

## ARTICLE INFO

### Article history:

Received 5 May 2014

Received in revised form

23 June 2014

Accepted 9 July 2014

Available online 24 July 2014

### Keywords:

Lithium iron phosphate

Polymer pyrolysis

Polytetrafluoroethylene

Carbon coating

Solid state synthesis

## ABSTRACT

Herein we report a facile and efficient solid state synthesis of carbon coated lithium iron phosphate ( $\text{LiFePO}_4/\text{C}$ ) cathode material achieved through the pyrolysis of polytetrafluoroethylene (PTFE). The current investigation is comparatively analyzed with the results of the composites of  $\text{LiFePO}_4/\text{C}$  (LFP/C) synthesized using polystyrene-block-polybutadiene (PS-*b*-PBD), polyethylene (PE) and sucrose as carbon precursors. The optimized LFP/C<sub>PTFE</sub> composite is synthesized at 700 °C using 10 wt.% PTFE. The composite exhibits remarkable improvement in capacity, cyclability and rate capability compared to those of LFP/C synthesized using (PS-*b*-PBD), PE and sucrose. The specific discharge capacities as high as 166 mA h g<sup>-1</sup> (theoretical capacity: 170 mA h g<sup>-1</sup>) at 0.2 C and 114 mA h g<sup>-1</sup> at 10 C rates were achieved with LFP/C<sub>PTFE</sub>. In addition, the composite exhibits a long-term cycling stability with the capacity loss of only 11.4% after 1000 cycles. PTFE shifts the size distribution of the composite to nanometer scale (approximately 120 nm), however the addition of sucrose and other polymers do not have such an effect. According to TEM and XPS analysis, LFP/C<sub>PTFE</sub> particles are mostly coated with a few nanometers thick carbon layer forming a core-shell structure. Residual carbon does not contain fluorine.

© 2014 Elsevier B.V. All rights reserved.

## 1. Introduction

Lithium ion battery technology has been applied in many portable electronic devices, electric/hybrid vehicles and stationary energy storage systems for storing solar and wind power as the most promising sustainable energy storage solution [1,2]. Among several cathode materials olivine-type  $\text{LiFePO}_4$  (LFP) is one of the most widely studied and generally considered to be a promising battery materials used in Plug-in Hybrid Electric Vehicle/Electric Vehicle (PHEV/EV) [1,3,4]. Besides the advantages of this material, such as low cost, high thermal and cycling stability, low toxicity and

relatively high theoretical capacity (170 mA h g<sup>-1</sup>), unfortunately, low electronic conductivity and slow diffusion of lithium ions across the two-phase boundary of LFP seriously limit its rate capability [5,6]. To overcome these problems, several strategies have been implemented including particle size minimization [7,8], doping with supervalent cations [9], carbon nanocoating [10–13] or carbothermal formation of the surface conducting phase [5,6,8,14,15]. To date, carbon coating (LFP/C) has been one of the most commonly used method to improve the specific capacity, rate capacity and cycling performance of LFP [5,6,8]. Depending on the pyrolysis behavior of carbon precursor, suppressing of the particle growth leading to both particle size minimization and intimate carbon contact can occur as an enhancement factor for the performance of LFP [8,16]. However, it is quite difficult to obtain a homogeneously coated carbon shell on LFP particles during the

\* Tel.: +90 262 677 2772; fax: +90 262 677 2309.

E-mail addresses: [ercan.avci@tubitak.gov.tr](mailto:ercan.avci@tubitak.gov.tr), [eavci07@yahoo.com](mailto:eavci07@yahoo.com).

heat treatment. In case of partial formation of carbon shell, an insufficient electronically conducting network would lead to decrease in the rate capability of the material.

There are mainly two methods for carbon coating of LFP particles. One is direct mixing of various particulate carbon materials, such as carbon nanomaterials (graphene, carbon nanotube, etc.) by mechanical means [6,17], but mostly leading non-uniform carbon coating. The other method is *in situ* deposition by using the pyrolysis of a carbon precursor, which usually results in more uniform coating compared to the previous method [6]. Previous studies for *in situ* carbon coating have mostly focused on the synthesis of LFP/C composite materials by using low weight organic precursors [18], such as sucrose, glucose or citric acid as the carbon source. Although the polymer pyrolysis method is a relatively simple and effective way to form carbon-coated materials, it has been rarely applied for coating the LFP particles [8,12,16]. In such a process, choosing a proper polymer precursor is an important step to obtain reduced size of LFP/C particles coated uniformly with a few nanometers thick carbon layers [8,16].

In this regard, recently, it was reported that an efficient solid state synthesis of carbon and nitrogen coated high performance  $\text{LiFePO}_4/\text{CN}$  was achieved via polymer pyrolysis method at  $700^\circ\text{C}$  [8]. It was claimed that PANI was leading to restrict the LFP particle growth by crosslinking of the polymer during the pyrolysis. The specific discharge capacities as high as  $164\text{ mA h g}^{-1}$  at  $0.1\text{ C}$  and  $100\text{ mA h g}^{-1}$  at  $10\text{ C}$  rates were achieved with  $\text{LiFePO}_4/\text{CN}$  particles, which are mostly coated with a few nanometers thick C–N layer. In another report, Nien and Chen [19] prepared LFP/C samples formed by calcinating amorphous LFP in the presence of various polymers such as polystyrene, polyethylene oxide, polybutadiene at  $600^\circ\text{C}$ . They reported that polystyrene (5 wt.%) derivative with functionalized aromatic groups exhibited an improved performance. They achieved a capacity of  $147\text{ mA h g}^{-1}$  and  $90\text{ mA h g}^{-1}$  at  $0.1\text{ C}$  and  $3\text{ C}$  rates, respectively. Additionally, Yu and Fang [20] announced that LFP/C composite prepared using polystyrene nano-spheres (7 wt.%) sintered at  $800^\circ\text{C}$  displayed a discharge capacity of  $167\text{ mA h g}^{-1}$  and  $150\text{ mA h g}^{-1}$  at  $0.1\text{ C}$  and  $1\text{ C}$ , respectively.

In this article, we introduce the polymers of polytetrafluoroethylene (PTFE), polyethylene (PE), polystyrene-block-polybutadiene (PS-*b*-PBD) and sucrose as carbon precursors for the solid state synthesis of LFP/C composites. Among the cathode materials synthesized at  $700^\circ\text{C}$  using 10 wt.% carbon precursors, LFP/C<sub>PTFE</sub> composite exhibits an outstanding electrochemical performance compared to others. PTFE restricts the size of LFP/C particles, however using PE, PS-*b*-PBD and sucrose as carbon precursors does not significantly influence it. Although fluorine doping [21,22] in the LFP/C<sub>PTFE</sub> was expected for the possible factor of high performance, no fluorine footprint was observed by XPS measurements. A mixture of nanometer and micrometer size LFP/C<sub>PTFE</sub> particles is formed as a result of the pyrolysis of PTFE. This composite seems to meet the need of excellent capacity retention and high performance in the power system for electric vehicles and stationary-storage applications.

## 2. Experimental

### 2.1. Synthesis of $\text{LiFePO}_4/\text{C}$ composites

As the starting materials for the solid-state synthesis, stoichiometric amounts of analytical grade  $2.24\text{ g}$  of  $\text{Li}_2\text{CO}_3$  (Alfa-Aesar),  $10.99\text{ g}$  of  $\text{FeC}_2\text{O}_4 \cdot 2\text{H}_2\text{O}$  (Aldrich),  $6.98\text{ g}$  of  $(\text{NH}_4)_2\text{HPO}_4$  (Carlo-Erba) as well as  $2.25\text{ g}$  of polystyrene-block-polybutadiene (PS-*b*-PBD, Aldrich), polyethylene (PE, Alfa-Aesar), polytetrafluoroethylene (PTFE, Alfa-Aesar) or sucrose (Carlo-Erba) as carbon source precursors were thoroughly planetary milled in mortar for  $2\text{ h}$

(300 rpm) in the mixture of different solvents. For all LFP/C samples, 10 wt.% of carbon precursors were used. Depending on the precursor used the following solvent mixtures (50 ml) were prepared; ethanol and toluene (1:1 v/v) mixture to dissolve PE and PS-*b*-PBD was heated at  $120^\circ\text{C}$  for  $1\text{ h}$ , ethanol and N-methylpyrrolidine (NMP, Merck) (1:1 v/v) mixture for PTFE and ethanol for sucrose. The resulting gel was dried at  $100^\circ\text{C}$  in a furnace and then heated to  $350^\circ\text{C}$  for  $6\text{ h}$  in Ar atmosphere. The decomposed mixture was pressed into pellets and sintered under Ar flow at  $700^\circ\text{C}$  for  $12\text{ h}$  in order to obtain the crystalline phase composites. The cathode materials prepared using PS-*b*-PBD, PE, PTFE and sucrose were donated as LFP/C<sub>PS-*b*-PBD</sub>, LFP/C<sub>PE</sub>, LFP/C<sub>PTFE</sub> and LFP/C<sub>sucrose</sub>, respectively as shown in Table 1.

### 2.2. Characterization of cathode materials

The crystallographic structural characterization was performed by X-ray powder diffraction. XRD of the LFP/C composites was carried out on a Rigaku Miniflex 600 diffractometer equipped with  $\text{Cu-K}\alpha$  radiation of  $\lambda = 0.15405\text{ nm}$  in the range of  $0^\circ < 2\theta < 80^\circ$ . The micromorphology of the LFP/C powders was observed using a JEOL JSM6510-LV scanning electron microscope (SEM). Transmission electron microscopy (TEM) measurements were performed using JEOL JEM 2100 HRTEM operating at  $200\text{ kV}$  (LaB<sub>6</sub> filament) with energy dispersive spectroscopy (EDS) systems. The carbon content was estimated using thermogravimetric analysis method (Mettler-Toledo TGA-851). Particle size analysis (PSA) of the composites was investigated by dispersing the materials in water using Malvern Mastersizer-2000. X-ray photoelectron spectroscopy (XPS) measurements were obtained using SPECS GmbH PHOIBOS-150 X-ray photoelectron spectrometer with monochromatic  $\text{Al K}\alpha$  ( $1486.6\text{ eV}$ ).

### 2.3. Cell fabrication and electrochemical measurements

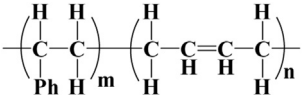
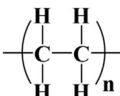
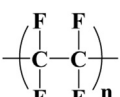
The crystalline cathode active materials of LFP/C were mixed and grounded with Super P (12 wt.%, Timcal Co.) and polyvinylidene fluoride (PVdF, 8 wt.%) as a binder dissolving in NMP for  $30\text{ min}$ . The resulting mixture was casted uniformly onto an aluminum foil and dried at  $100^\circ\text{C}$ . Electrodes were punched in the form of a disc having  $5\text{--}7\text{ mg cm}^{-2}$  of active material, pressed and dried at  $100^\circ\text{C}$  for  $4\text{ h}$ . The coin cells (CR2032) were assembled in an argon-filled glove-box (Vigor) with a Li metal disc as anode and Whatman GF/D glass-fiber as separator and  $1\text{ M LiPF}_6$  in a mixture of ethylene carbonate (EC) and diethyl carbonate (DEC) (1:1 in vol. ratio) as the electrolyte. Cyclic voltammograms (CV) (between  $2.0$  and  $4.3\text{ V}$ ) and galvanostatic charge/discharge measurements were carried out (between  $2.2$  and  $4.2\text{ V}$ ) with PAR VersaSTAT Multi channel potentiostat/galvanostat.

## 3. Results and discussion

### 3.1. Material characterization

The crystal structures of LFP/C powders prepared using the carbon precursors of PS-*b*-PBD, PE, PTFE and sucrose were confirmed by X-ray diffraction (XRD) (Fig. 1). All peaks on each curve can be indexed as a single phase with an ordered orthorhombic olivine structure with a space group  $Pmnb$  (ICDD (PDF-2/Release 2011 RDB) DB card number: 01-074-9597) indicating the successful synthesis of phase-pure  $\text{LiFePO}_4$  (lattice parameters:  $a = 10.323\text{ \AA}$ ,  $b = 6.007\text{ \AA}$ ,  $c = 4.689\text{ \AA}$ ,  $\pm 0.003\text{ \AA}$  depending on the materials). There were no obvious diffraction peaks corresponding to other impurity peaks such as  $\text{Li}_3\text{PO}_4$ ,  $\text{Fe}_2\text{P}$ . This reveals that the carbon coating did not result in any change in crystal structure of

**Table 1**  
Carbon precursors of PS-*b*-PBD, PE, PTFE and sucrose and residual carbon content of LFP/C composites.

Carbon source			Notation (material/ carbon source)	Final carbon content (wt.%)	Loss in carbon source (wt.%)
Material	Physical properties	Melting point (°C)			
Polystyrene-block-Polybutadiene (PS- <i>b</i> -PBD) 	Granule, 30 wt.% styrene, 80% diblock	230–240	LFP/C <sub>PS-<i>b</i>-PBD</sub>	7.3	71
Polyethylene (PE) 	Powder, 500 μm, low density	125	LFP/C <sub>PE</sub>	4.5	82
Polytetrafluoroethylene (PTFE) 	Powder, 6–10 μm	327	LFP/C <sub>PTFE</sub>	9.8	61
Sucrose C <sub>12</sub> H <sub>22</sub> O <sub>11</sub>		None, decom-poses at 186	LFP/C <sub>sucrose</sub>	9.1	64

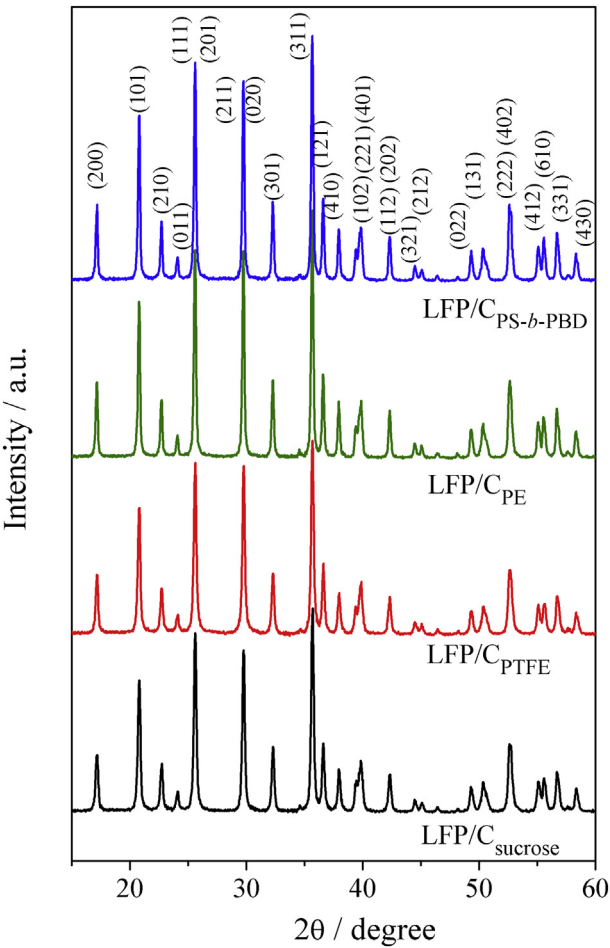


**Fig. 1.** XRD patterns of LFP/C composites synthesized using PS-*b*-PBD, PE, PTFE and sucrose as carbon sources.

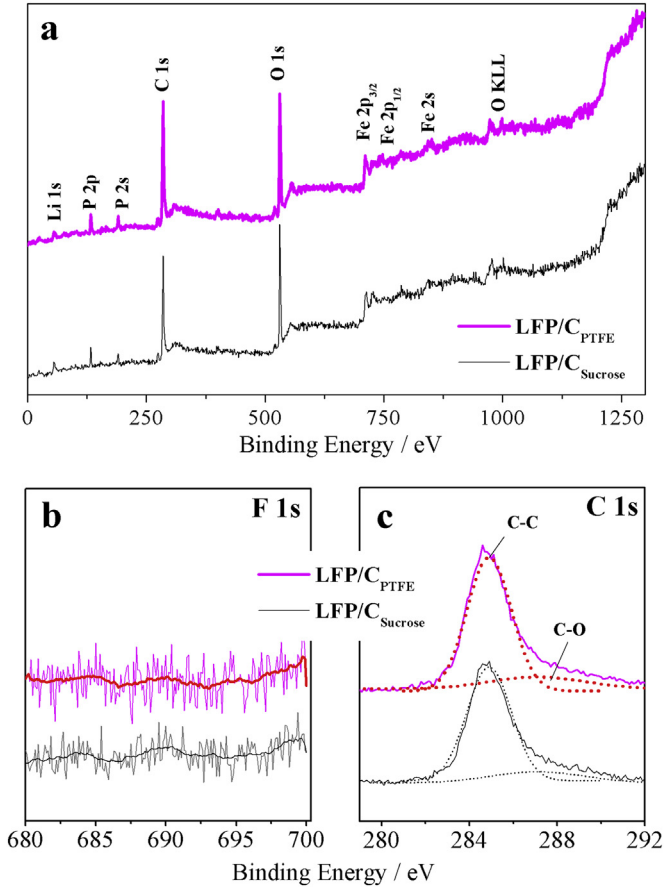


**Fig. 2.** X-ray photoelectron spectroscopy (XPS) spectra of LFP/C composites synthesized using PTFE (red) and sucrose (black) as carbon sources. Survey spectra (a), the high-resolution F 1s spectra (b) and C 1s spectra (c) (For interpretation of the references to color in this figure legend, the reader is referred to the web version of this article.).

LFP/C samples. The absence of any graphite peak was attributed to the amorphous state of carbon [23]. Crystallite sizes calculated according to Williamson–Hall method vary between 23 and 28 nm. These results reflect that a simple solid state synthesis method can produce carbon coated LiFePO<sub>4</sub> with well crystallinity and the purity, which are key factors for high-performance cathode material.

The surface compositions of LFP/C<sub>PTFE</sub> and LFP/C<sub>sucrose</sub> composites synthesized using PTFE and sucrose, respectively, were investigated via X-ray photoelectron spectroscopy (XPS) measurements (Fig. 2). The survey spectra of both samples are shown in Fig. 2(a). The binding energy (BE) is referenced by setting the O 1s BE to 531.5 eV considering the report of H. Liu et al. [24]. The BE peaks observed at 711.3 eV (Fe 2p) correspond only to the Fe<sup>2+</sup> valence state for both of samples. The peaks representing the other valence state of iron cannot be seen. The peak P 2p, which is composed of +5 valences, is observed at 133.8 eV. The peaks at 55.8 eV demonstrate the presence of Li at both samples. Absence of a clear peak around 689.0 eV [25] in high resolution F 1s spectrum of LFP/C<sub>PTFE</sub> composite,

surprisingly, indicates that there is no fluorine (F) originated from PTFE carbon precursor (Fig. 2(b)). The fitting of high resolution C 1s spectra shown in Fig. 2(c) is resolved into two peaks at 284.7 eV and 287.1 eV indicating the presence of –C–C bonding and –C–O bonding, respectively [24,26]. The presence of –C–O bonding indicates the existence of a strong interaction between the carbon shell and the oxygen of LiFePO<sub>4</sub> molecule in both LFP/C<sub>sucrose</sub> and LFP/C<sub>PTFE</sub> composites.

All those XPS results obviously show that there is no fluorine (F) in the structure of cathode material originating from the decomposition of PTFE. This is the indication of complete removal of F atoms from PTFE during the synthesis of LFP/C<sub>PTFE</sub>. It is most likely that the pyrolysis characteristic of PTFE differs in the presence of new-born LiFePO<sub>4</sub> material, which probably catalyzes the breaking of strong C–F bond in the PTFE backbone at high temperatures.

The carbon precursors of PS-*b*-PBD, PE, PTFE and sucrose were thermally analyzed in order to examine the effect of their pyrolysis on the formation of LFP/C composites as shown in Fig. 3(a). The samples were heated from 25 °C to 900 °C at a rate of 10 °C min<sup>−1</sup> under N<sub>2</sub> flow (40 ml min<sup>−1</sup>). The pyrolysis of all carbon precursors take place at single step starting at 200 °C, 330 °C, 400 °C and 500 °C for sucrose, PS-*b*-PBD, PE, and PTFE, respectively. Sucrose loses 75% of its weight till 700 °C. On the other hand, the pristine polymers decompose and lose their weight completely till 600 °C.

According to the literature about the thermogravimetric analysis of the polymers, PS-*b*-PBD, PE and PTFE decompose as a result of the mechanism initiated by random chain scission, followed by depolymerization of and intramolecular hydrogen transfer. The main pyrolysis products of PS-*b*-PBD are ascribed as toluene,  $\alpha$ -methylstyrene, ethylbenzene as well as light alkanes and alkenes [27,28]. The decomposition products of PE include a wide range of alkanes and alkenes. The principal pyrolysis products of PTFE are the monomer of polymer (C<sub>2</sub>F<sub>4</sub>) and C<sub>3</sub>F<sub>6</sub> as well as less amount of light ends (CF<sub>4</sub> and C<sub>2</sub>F<sub>6</sub>) and carbon black under inert atmosphere [29].

To understand the pyrolysis mechanism of carbon precursors during the synthesis of LFP/C composites, TGA was performed under N<sub>2</sub> atmosphere (Fig. 3(b)). All starting materials (Li<sub>2</sub>CO<sub>3</sub>, FeC<sub>2</sub>O<sub>4</sub>·2H<sub>2</sub>O, (NH<sub>4</sub>)<sub>2</sub>HPO<sub>4</sub>) in the presence of carbon precursors were mixed in appropriate solvents as described in the experimental part. After drying of mixtures in vacuum oven at 100 °C overnight, TGA was carried out. The same heating procedure with the LFP/C synthesis was applied during TGA by holding at 350 °C (6 h) and at 700 °C (10 h). The first step (I) at the temperatures up to 160 °C, all mixtures lose some amount of unbound water

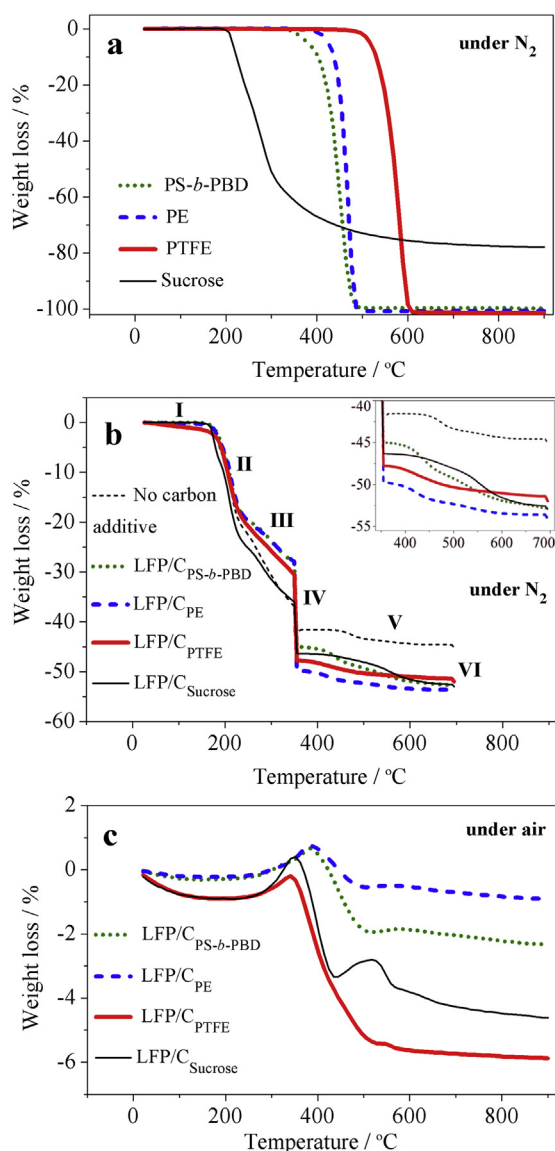


**Fig. 3.** Thermogravimetric curves of PS-*b*-PBD, PE, PTFE and sucrose under N<sub>2</sub> atmosphere (a), of the mixtures of starting materials to synthesize the different LFP/C samples in the presence of carbon precursors (waiting 6 h at 350 °C and 10 h at 700 °C) under N<sub>2</sub> (b) and of LFP/C composites synthesized using PS-*b*-PBD, PE, PTFE and sucrose as carbon sources under air (c).

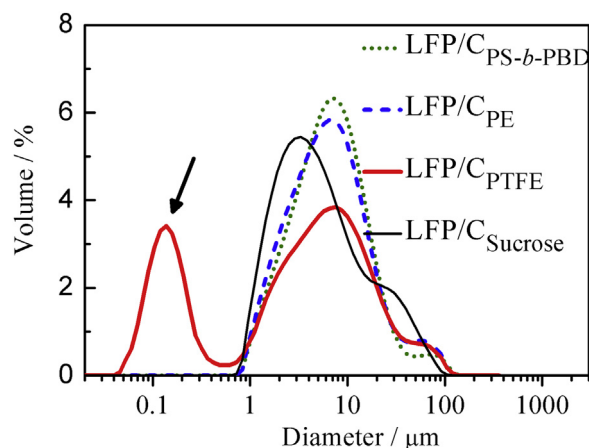


**Fig. 4.** Particle size distributions of different LFP/C composites synthesized using PS-*b*-PBD, PE, PTFE and sucrose as carbon sources.



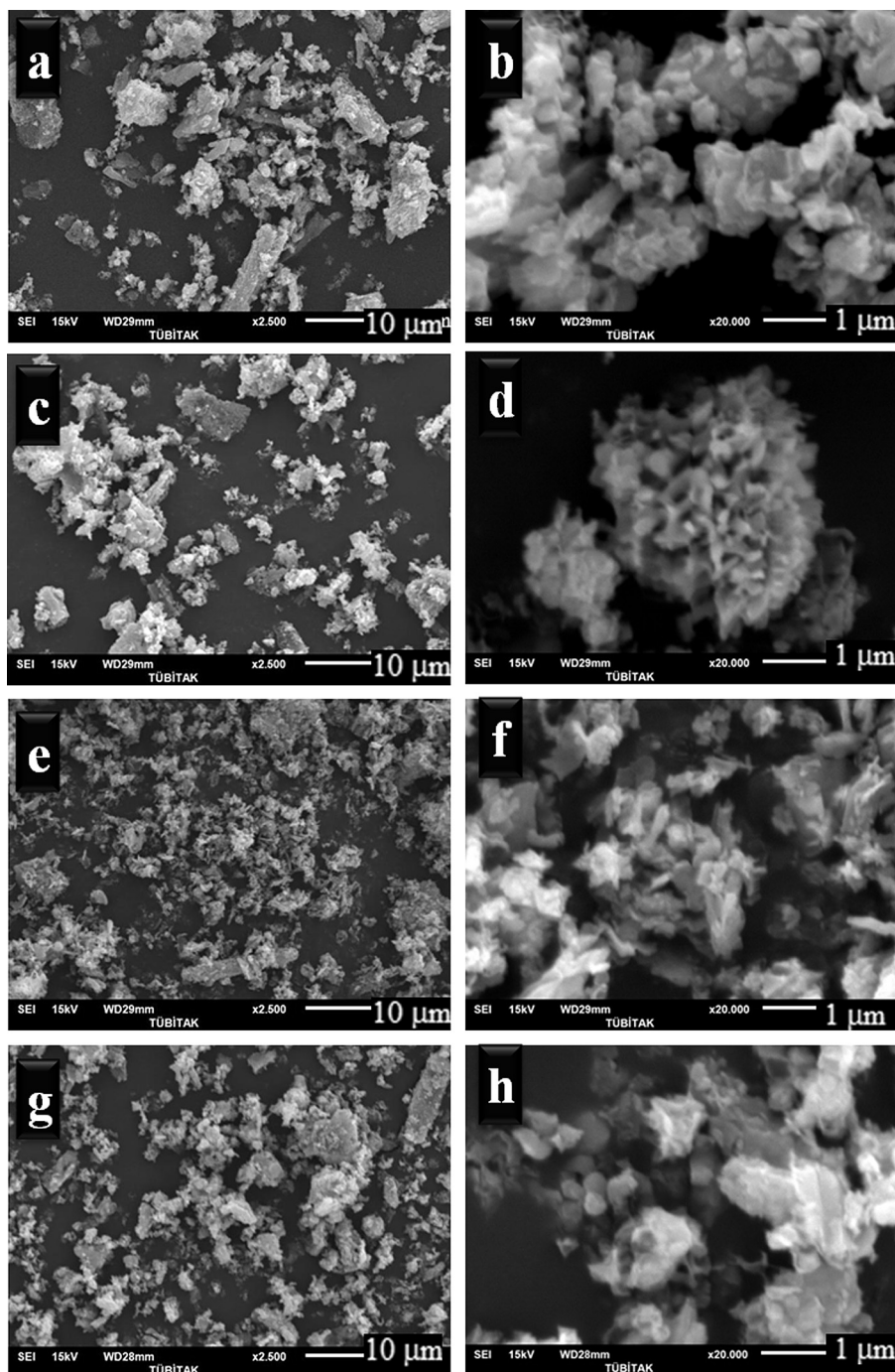


**Fig. 5.** SEM images of (a,b) LFP/C<sub>PS-B-PBD</sub>, (c,d) LFP/C<sub>PE</sub>, (e,f) LFP/C<sub>PTFE</sub>, (g,h) LFP/C<sub>sucrose</sub> composites sintered at 700 °C.

(1–3 wt.%). The second and third steps (II, III) in the temperature range of 160 °C and 350 °C are attributed to the loss of ammonia and bound water (26–29 wt.%) for all mixtures [8], as well as, partial loss of sucrose. At the fourth step (IV, waiting 350 °C), all mixtures undergo calcinations and LiFePO<sub>4</sub> particles are formed. During this heating period, the decomposition of polymers is not expected in significant level, whereas sucrose is decomposed partially. The weight loss at the fifth and last steps (V, VI, inset in Fig. 3(b)) between 350 °C and 700 °C, the decomposition of polymers and sucrose is completed. Specifically, investigation within these temperature range is important to clarify the decomposition of PTFE during the synthesis of carbon coated LFP. For LFP/C<sub>PTFE</sub>

material, the weight loss during these periods is about 5 wt.%, which most probably corresponds to the loss of all fluorine atoms of PTFE.

To quantify the carbon content in the LFP/C composites, thermogravimetric analysis (TGA) was carried out under air (40 ml min<sup>-1</sup>) at a heating rate of 10 °C min<sup>-1</sup> (Fig. 3(c)). The slight weight loss between room temperature and 350 °C is varying in the range of 0.4 and 1.1% depending on the composites, which corresponds to the evaporation of adsorbed moisture in the samples. Whereas, the weight gain observed at temperature ranges between 350 and 500 °C is the result of the oxidation of Fe(II) to Fe(III) (formation of iron oxides), which is about 4.8 wt.% [30]. Considering

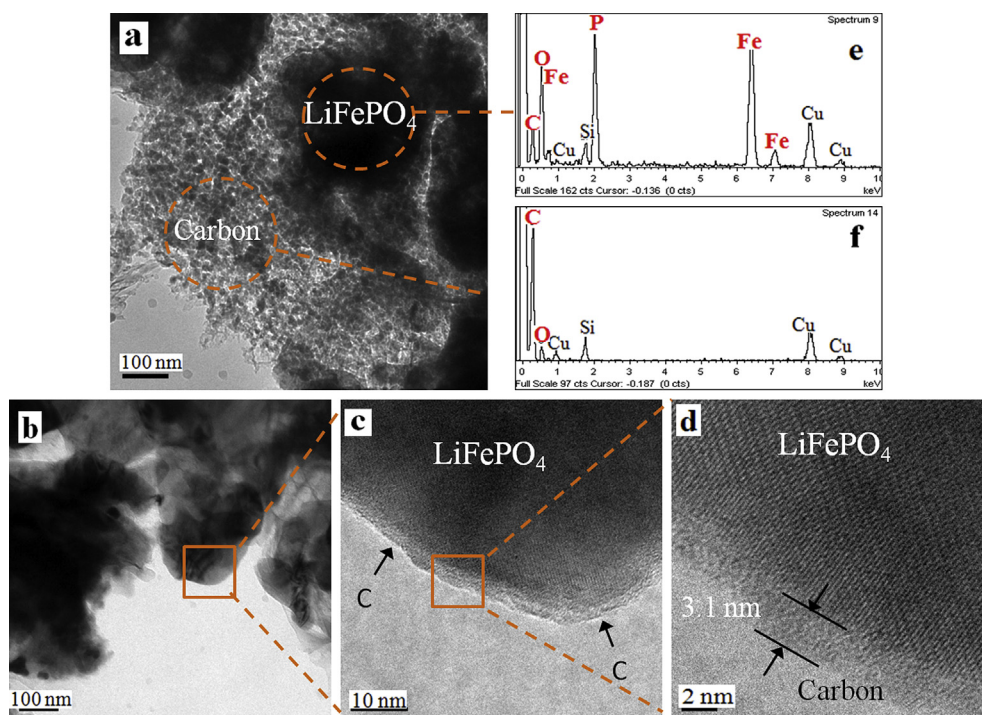


**Fig. 6.** (a–d) TEM and HRTEM images of LFP/C<sub>sucrose</sub> composite particles; (e,f) EDS patterns for the particles.

this increment in TGA results, carbon contents of LFP/C<sub>PS-b-PBD</sub>, LFP/C<sub>PE</sub>, LFP/C<sub>PTFE</sub> and LFP/C<sub>sucrose</sub> were calculated as 7.3, 4.5, 9.8 and 9.1 wt.%, respectively. The residual carbon originating from the polymers in the structure of LFP/C materials clearly indicates that

the pyrolysis products do not extinct completely as opposed to the TGA plots of pristine polymers alone (Fig. 3(a)).

It is also worth noting that the weight loss of carbon precursors during the active material preparation can be calculated as ~71 wt.%

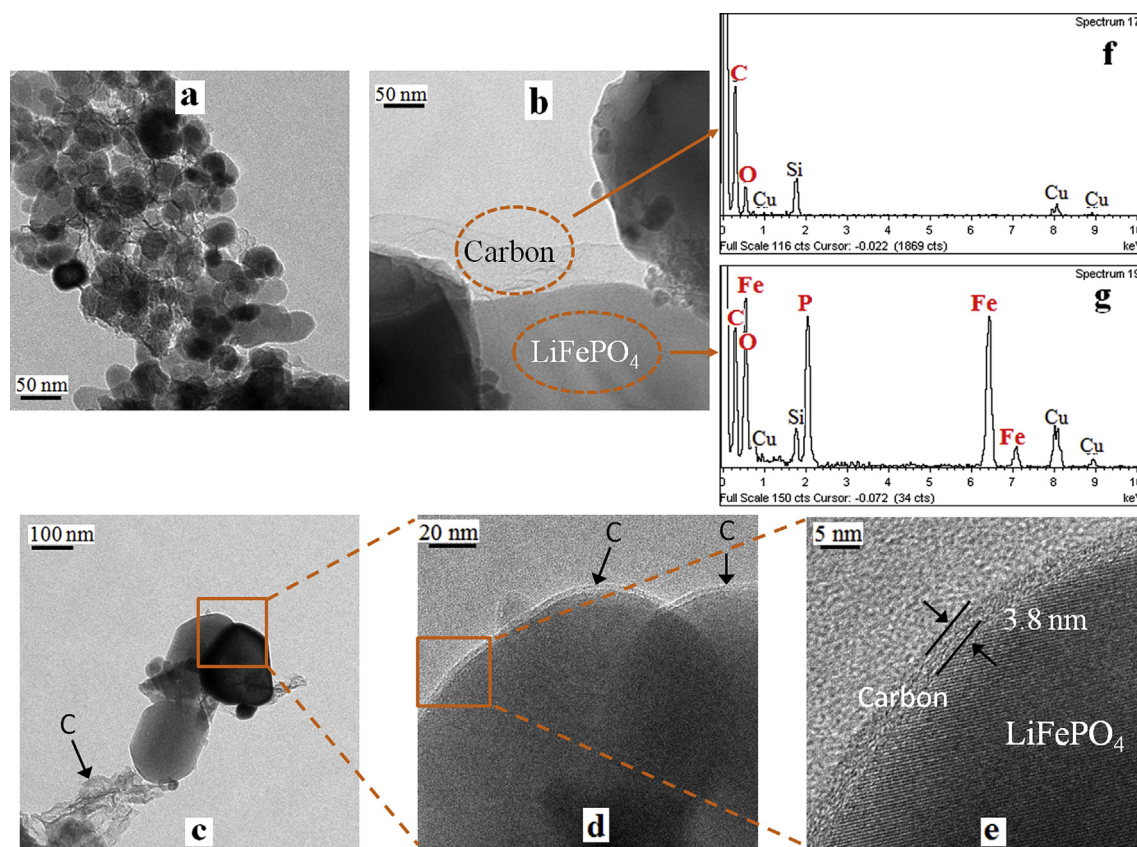


**Fig. 7.** (a–e) TEM and HRTEM images of LFP/C<sub>PTFE</sub> composite particles; (f,g) EDS patterns for the particles.



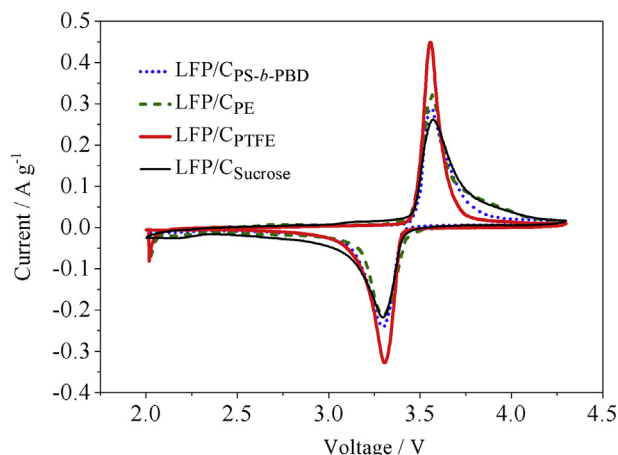


Fig. 8. CV curves of different LFP/C composites synthesized using PS-*b*-PBD, PE, PTFE and sucrose as carbon sources at scan rate of  $0.1 \text{ mV s}^{-1}$ .

for LFP/C<sub>PS-*b*-PBD</sub>, ~82 wt.% for LFP/C<sub>PE</sub>, ~61 wt.% for LFP/C<sub>PTFE</sub> and ~64 wt.% for LFP/C<sub>sucrose</sub>, as compared to the initial weight of substances. Specifically, for the composite of LFP/C<sub>PTFE</sub>, it is interesting that the amount of residual carbon is very close to the amount of carbon existing in PTFE structure ( $(\text{C}_2\text{F}_4)_n$ ). In more detail, despite of the amount of carbon in pristine PTFE is 40 wt.%, interestingly, the residue of carbon in LFP/C<sub>PTFE</sub> is 39 wt.%. All these findings indicate that the carbon precursors, except PTFE, lose most of their weight as a result of the volatilization of light hydrocarbon products, whereas PTFE loses only fluorine during the synthesis and almost all carbon remains in the structure of cathode material considering the XPS results.

Particle size distribution measurements for LFP/C samples using a Mastersizer 2000 demonstrate the interesting behavior of LFP/C<sub>PTFE</sub> compared to other LFP/C samples (Fig. 4). As the distribution curves of LFP/C samples prepared using PS-*b*-PBD, PE or sucrose are centered at a single region around 4–10  $\mu\text{m}$ , surprisingly, the distribution for LFP/C<sub>PTFE</sub> composite is localized at two regions; one is centered around 120 nm (~40 v/v%) and the other is at ~10  $\mu\text{m}$  (~60 v/v%). The distributions clearly reveal that PTFE restricts the growth of the composite particles.

The morphology of the LFP/C composites was characterized by SEM as shown in Fig. 5. All SEM pictures present irregular shaped particles of LFP/C with agglomeration in varying degrees

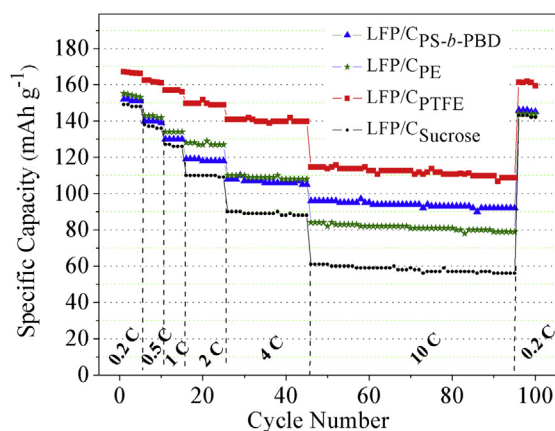


Fig. 9. Rate capability of different LFP/C composites synthesized using PS-*b*-PBD, PE, PTFE and sucrose as carbon sources.

(Fig. 5(a–h)). It is obvious that LFP/C<sub>PTFE</sub> (Fig. 5(e,f)) consists of particles much smaller than other LFP/C composites. Both SEM and PSA results reveal that carbon coating via pyrolysis of PTFE plays an important role in controlling the growth of particles. The reduced particle size results in shortening of the diffusion path of  $\text{Li}^+$  and hence better electrochemical performance of LFP/C<sub>PTFE</sub> compared to other LFP/C samples. This is further supported by the electrochemical measurements described below.

In order to check the carbon distribution in LFP/C<sub>PTFE</sub> and LFP/C<sub>sucrose</sub> powders, high resolution-transmission electron microscopy (HR-TEM) and energy dispersive spectroscopy (EDS) methods were utilized (Figs. 6 and 7). There are discrete carbon layers coating on both LFP particles as shown in Figs. 6(a–d) and 7(a–e). The partial surface of particles is coated with a carbon layer of less than 100 nm thickness. One of the common features of the TEM images of both samples is that large carbon segments are located between large LFP particles (Figs. 6(a) and 7(b)). The images at higher magnification (Figs. 6(c,d) and 7(d,e)) demonstrate that the coating is extended over the surfaces of LFP particles forming a core-shell structure. Thicknesses of the shells are measured as 3.1 nm and 3.8 nm for the samples of LFP/C<sub>sucrose</sub> and LFP/C<sub>PTFE</sub>, respectively. The complete carbon coating around or between the particles is expected to contribute to the improved electrochemical properties of the composites. EDS elemental mapping of C, Fe, P and O in LFP/

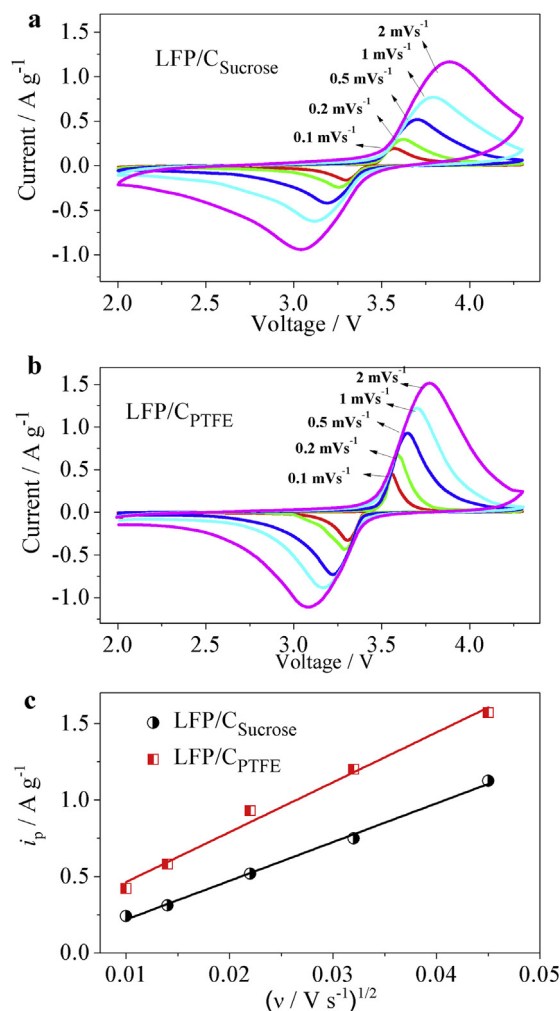


Fig. 10. CV curves of (a) LFP/C<sub>sucrose</sub> and (b) LFP/C<sub>PTFE</sub> at various scan rates. (c) The relationship of peak current ( $i_p$ ) and the square root of scan rate ( $v^{1/2}$ ) for both samples.

C<sub>PTFE</sub> composite showed the existence of those elements in the structure but not fluorine.

Evaluating the results derived from PSA, XPS, TGA and TEM methods, the possible explanation for the formation of nano-sized carbon coated LiFePO<sub>4</sub> particles by using PTFE as carbon precursor can be given as follows. First, it is clear that the pyrolysis behavior of PTFE in the presence LFP synthesis starting materials differs from that of the pure form of it. XPS and XRD results show that there is no fluorine (F) containment either in the shell or crystal structure of LFP/C<sub>PTFE</sub> particle. The shell contains only carbon species.

### 3.2. Electrochemical measurements

Fig. 8 shows the cyclic voltammogram (CV) curves of LFP/C synthesized using PS-*b*-PBD, PE, PTFE and sucrose precursors scanned at a rate of 0.1 mV s<sup>-1</sup>. All samples reveal the single-electron reaction mechanism indicating the characteristic redox behavior of LiFePO<sub>4</sub> cathode material. In comparison with LFP/C samples prepared using PS-*b*-PBD, PE and sucrose, LFP/C<sub>PTFE</sub> sample has the sharpest redox peaks which indicate the high rate capability of the material.

Fig. 9 demonstrates the cyclability performances of LFP/C electrodes at the discharging rate ranging from 0.2 C to 10 C

(1 C = 170 mA g<sup>-1</sup>). In comparison to LFP/C composites synthesized using PS-*b*-PBD, PE and sucrose, LFP/C<sub>PTFE</sub> composite demonstrates a promising capacity, cyclability, and rate performance. The specific discharge capacities as high as 166 mA h g<sup>-1</sup> at 0.2 C (approximating the theoretical value of 170 mA h g<sup>-1</sup>), 114 mA h g<sup>-1</sup> at 10 C rates with a 3% of capacity fading after 100 cycles were obtained for LFP/C<sub>PTFE</sub>. On the other hand, LFP/C composites synthesized using PS-*b*-PBD, PE and sucrose exhibit relatively close discharge capacities to that of LFP/C<sub>PTFE</sub> at lower rates (around 150 mA h g<sup>-1</sup> at 0.2 C). At higher rates, the specific discharge capacities differ from each other. LFP/C<sub>PS-*b*-PBD</sub>, LFP/C<sub>PE</sub> and LFP/C<sub>sucrose</sub> give the capacities of 96, 84 and 62 mA h g<sup>-1</sup> at 10 C, respectively. For these three samples, at the end of 100 charge–discharge cycles around 6% of capacity fading was measured. The excellent electrochemical performance of LFP/C<sub>PTFE</sub> implies that the coating of LFP surface with pyrolyzed PTFE facilitates the electrochemical insertion/extraction process of Li<sup>+</sup> ion, especially at high rate.

Cyclic voltammetry was used to examine the kinetics of lithium intercalation and de-intercalation. Fig. 10(a,b) shows the CV curves of LFP/C<sub>sucrose</sub> and LFP/C<sub>PTFE</sub> at an increasing scan rate from 0.1 to 2 mV s<sup>-1</sup>, respectively. It is clear that the intensity and the area under the redox peaks for both composites increase with the scan rate. Using Randles–Sevcik equation [31],  $i_p = 2.69 \times 10^5 n^{3/2} A D^{1/2} C \nu^{1/2}$ , the linear dependence of peak current ( $i_p$ ) of CV of samples on the square root of scan rate ( $\nu^{1/2}$ ) can be observed in Fig. 11(c). Considering the parameters of  $A$  (electrode area),  $C$  (concentration of Li<sup>+</sup>) and  $n$  (number of electrons involved in the redox process) are fixed values for both electrodes, the diffusion coefficient of lithium ( $D_{Li}$ ) of LFP/C<sub>PTFE</sub> is found to be 1.3 times higher than that of LFP/C<sub>sucrose</sub>. This designates that the particle size reduction in LFP/C<sub>PTFE</sub> material possibly improves transportation of Li ions during cell operation.

Fig. 11(a,b) demonstrates the galvanostatic charge–discharge voltage profiles of cells containing LFP/C<sub>sucrose</sub> and LFP/C<sub>PTFE</sub> at the increasing rate from 0.2 C to 10 C between 2.2 and 4.2 V vs. Li<sup>+</sup>/Li. Both samples exhibit typical flat charge–discharge plateaus at approximately 3.4 V implying the Fe<sup>2+</sup>/Fe<sup>3+</sup> redox reaction. As shown in Fig. 11(a), the initial discharge capacity of LFP/C<sub>sucrose</sub> is around 150 mA h g<sup>-1</sup> at 0.2 C rate, whereas LFP/C<sub>PTFE</sub> exhibits a higher discharge capacity of 166 mA h g<sup>-1</sup> at the same condition. At higher C-rates, again LFP/C<sub>PTFE</sub> composite demonstrates a superior performance compared to the LFP/C<sub>sucrose</sub> sample. As shown in Fig. 11(c), it is clear that the composite of LFP/C<sub>PTFE</sub> demonstrates a slower enlargement in voltage polarization compared to the LFP/C<sub>sucrose</sub> composite as the C-rate rises.

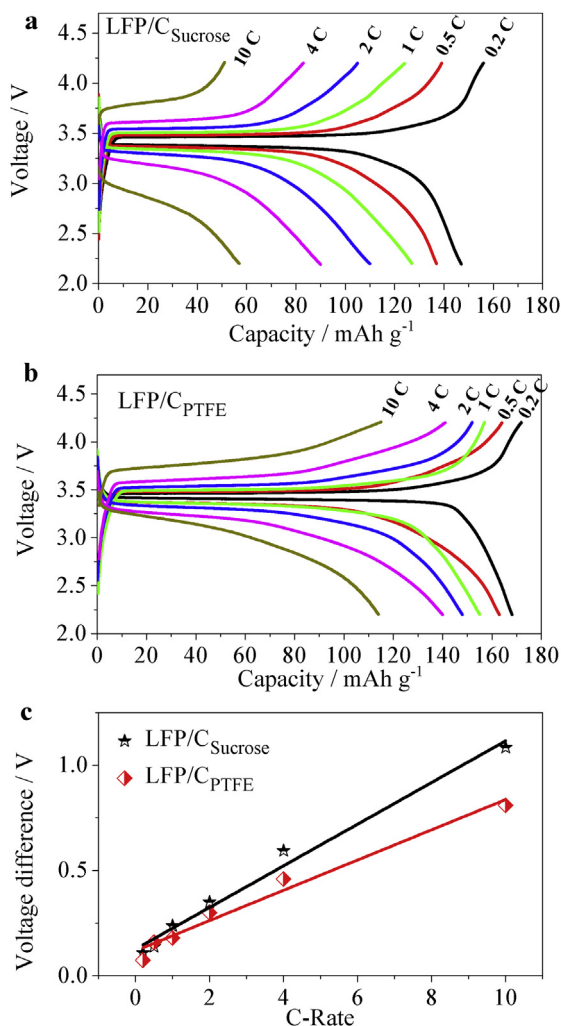


Fig. 11. Charge–discharge profiles of (a) LFP/C<sub>sucrose</sub> and (b) LFP/C<sub>PTFE</sub> composites. (c) The dependence of voltage difference between charging and discharging at half capacity on C-rate for both samples.

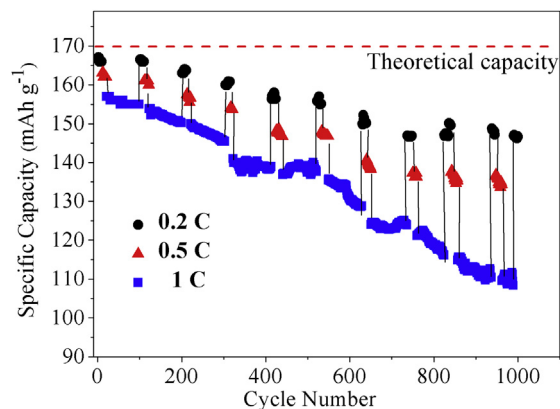


Fig. 12. Cyclability performance (1000 cycles) of LFP/C<sub>PTFE</sub> synthesized using 10 wt.% PTFE as carbon precursor.



Long term cycling capability of LFP/C<sub>PTFE</sub> sample is tested at different C-rates as shown in Fig. 12. The initial discharge capacity of the composite is 166 mA h g<sup>-1</sup> at 0.2 C and found to decay gradually with continuous cycling at varying rates, retaining 147 mA h g<sup>-1</sup> at 0.2 C after 1000 cycles suffering only 11.4% capacity loss. Such a superior electrochemical performance surely can satisfy the power requirements of electric or hybrid electric vehicles [32].

#### 4. Conclusions

A simple and low-cost solid state synthesis method was followed to prepare the mixture of nanometer and micrometer size LFP/C<sub>PTFE</sub> composite using PTFE as carbon precursor. Carbonization of PTFE possibly leads to size reduction and formation of complete carbon coating on LFP. LFP/C<sub>PTFE</sub> composite prepared using 10 wt.% PTFE and sintered at 700 °C, contains 9.8 wt.% carbon. PTFE leads to the shifting of the size distribution to nanometer scale (approximately 120 nm), however the addition of sucrose and other polymers does not exhibit such a result. The LFP/C<sub>PTFE</sub> composite exhibits a higher electrochemical performance compared with LFP/C composites synthesized using PS-*b*-PBD, PE and sucrose. LFP/C<sub>PTFE</sub> particles are mostly covered with a few nanometers thick carbon layer, forming a core–shell structure. No fluorine is detected in the samples. The specific discharge capacities of 166 mA h g<sup>-1</sup> at 0.2 C, 114 mA h g<sup>-1</sup> at 10 C rates with a 3% of capacity fading after 100 cycles were achieved. Besides, the composite exhibits a long-term cycling stability with the capacity loss of only 11.4% after 1000 cycles.

#### Acknowledgments

The authors thank to The Scientific and Technological Research Council of Turkey (TUBITAK) for the financial support under the COST programme (contract no. 111T567). Thanks are also to the project manager Dr. Muhsin Mazman, M.Sc. Serkan Gürbüz for XRD measurements and M.Sc. Yeliz D. Çetin for TGA experiments.

#### References

- [1] O.K. Park, Y. Cho, S. Lee, H.C. Yoo, H.K. Song, J. Cho, *Energy Environ. Sci.* 4 (2011) 1621–1633.
- [2] D. Uzun, M. Doğrusöz, M. Mazman, E. Biçer, E. Avci, T. Şener, T.C. Kaypmaz, R.D. Çakan, *Solid State Ionics* 249–250 (2013) 171–176.
- [3] A.K. Padhi, K.S. Nanjundaswamy, J.B. Goodenough, *J. Electrochem. Soc.* 144 (1997) 1188–1194.
- [4] N. Terada, T. Yanagi, S. Arai, M. Yoshikawa, K. Ohta, N. Nakajima, N. Arai, *J. Power Sources* 1–2 (2001) 80–92.
- [5] B.L. Ellis, K.T. Lee, L.F. Nazar, *Chem. Mater.* 22 (2010) 691–714.
- [6] J. Wang, X. Sun, *Energy Environ. Sci.* 5 (2012) 5163–5185.
- [7] P. Gibot, M.C. Cabanas, L. Laffont, S. Levasseur, P. Carlach, S. Hamelet, J.M. Tarascon, C. Masquelier, *Nat. Mater.* 7 (2008) 741–747.
- [8] E. Avci, M. Mazman, D. Uzun, E. Biçer, T. Şener, *J. Power Sources* 240 (2013) 328–337.
- [9] H. Goktepe, H. Sahan, A. Ulgen, S. Patat, *J. Mater. Sci. Technol.* 27 (2011) 861–864.
- [10] Y. Wang, Y. Wang, E. Hosono, K. Wang, H. Zhou, *Angew. Chem., Int. Ed.* 47 (2008) 7461–7465.
- [11] W.M. Chen, L. Qie, L.X. Yuan, S.A. Xia, X.L. Hu, W.X. Zhang, Y.H. Huang, *Electrochim. Acta* 56 (2011) 2689–2695.
- [12] J. Liu, G. Yang, X. Zhang, J. Wang, R. Wang, *J. Power Sources* 197 (2012) 253–259.
- [13] S.Y. Chung, J.T. Blocking, Y.M. Chiang, *Nat. Mater.* 1 (2002) 123–128.
- [14] K. Yang, Z. Lin, X. Hu, Z. Deng, J. Suo, *Electrochim. Acta* 56 (2011) 2941–2946.
- [15] M. Mazman, Ö. Çuhadar, D. Uzun, E. Avci, E. Biçer, T.C. Kaypmaz, Ü. Kadiroğlu, *Türk. J. Chem.* 38 (2014) 297–308.
- [16] Y. Wang, Z. Liu, S. Zhou, *Electrochim. Acta* 58 (2011) 359–363.
- [17] Y. Long, Y. Shu, X. Ma, M. Ye, *Electrochim. Acta* 117 (2014) 105–112.
- [18] H. Goktepe, H. Sahan, F. Kilic, S. Patat, *Ionics* 16 (2010) 203–208.
- [19] Y.H. Nien, J.R. Carey, J.S. Chen, *J. Power Sources* 193 (2009) 822–827.
- [20] S. Yu, S. Dan, G. Luo, W. Liu, Y. Luo, X. Yu, Y. Fang, *J. Solid State Electrochem* 16 (2012) 1675–1681.
- [21] F. Pan, W.I. Wang, *J. Solid State Electrochem* 16 (2012) 1423–1427.
- [22] X.Z. Liao, Y.S. He, Z.F. Ma, X.M. Zhang, L. Wang, *J. Power Sources* 174 (2007) 720–725.
- [23] M. Zhang, B. Qu, D. Lei, Y. Chen, X. Yu, L. Chen, Q. Li, Y. Wang, T. Wang, *J. Mater. Chem.* 22 (2012) 3868–3874.
- [24] H. Liu, H. Yang, J. Li, *Electrochim. Acta* 55 (2010) 1626–1629.
- [25] D. Gong, Q. Xue, H. Wang, *Wear* 148 (1991) 161–169.
- [26] A. Fedorkova, R. Orinakova, A. Orinak, M. Kupkova, H.D. Wiemhöfer, J.N. Audinot, J. Guillot, *Solid State Sci.* 14 (2012) 1238–1243.
- [27] G. Audisio, F. Bertini, *J. Anal. Appl. Pyrolysis* 24 (1992) 61–74.
- [28] S.B. Munteanu, M. Brebu, C. Vasile, *Polym. Degrad. Stab.* 89 (2005) 501–512.
- [29] E. Meissner, A. Wroblewska, E. Milchert, *Polym. Degrad. Stab.* 83 (2004) 163–172.
- [30] S.F. Yang, Y.N. Song, P.Y. Zavalij, M.S. Whittingham, *Electrochem. Commun.* 4 (2002) 239–244.
- [31] B. Xu, M.L. Ye, Y.X. Yu, W.D. Zhang, *Anal. Chim. Acta* 674 (2010) 20–26.
- [32] E. Baker, H. Chon, J. Keisler, *Technol. Forecast. Soc.* 77 (2010) 1139–1146.